ELSEVIER

European Journal of Cardio-thoracic Surgery 22 (2002) 497–503

EUROPEAN JOURNAL OF CARDIO-THORACIC SURGERY

www.elsevier.com/locate/ejcts

A four-dimensional study of the aortic root dynamics

E. Lansac[a], H.S. Lim[b], Y. Shomura[c], K.H. Lim[b], N.T. Rice[c], W. Goetz[c], C. Acar[a], C.M.G. Duran[c,*]

[a]*The University of La Pitié-Salpetrière, Paris, France*
[b]*Nanyang Technological University, Singapore, Singapore*
[c]*The International Heart Institute of Montana Foundation at St. Patrick Hospital, The University of Montana, 554 West Broadway, Missoula, MT, 59802 USA*

Received 13 March 2002; received in revised form 14 June 2002; accepted 26 June 2002

Abstract

Objective: Although aortic root expansion has been well studied, its deformation and physiologic relevance remain controversial. Three-dimensional (3-D) sonomicrometry (200 Hz) has made time-related 4-D study possible. **Methods**: Fifteen sonomicrometric crystals were implanted into the aortic root of eight sheep at each base (three), commissures (three), sinuses of Valsalva (three), sinotubular junction (three), and ascending aorta (three). In this acute, open-chest model, the aortic root geometric deformations were time related to left ventricular and aortic pressures. **Results**: During the cardiac cycle, aortic root volume increased by mean ± 1 standard error of the mean (SEM) 33.7 ± 2.7%, with 36.7 ± 3.3% occurring prior to ejection. Expansion started during isovolumic contraction at the base and commissures followed (after a delay) by the sinotubular junction. At the same time, ascending aorta area decreased (−2.6 ± 0.4%). During the first third of ejection, the aortic root reached maximal expansion followed by a slow, then late rapid decrease in volume until mid-diastole. During end-diastole, the aortic root volume re-expanded by 11.3 ± 2.4%, but with different dynamics at each area level. Although the base and commissural areas re-expanded, the sinotubular junction and ascending aorta areas kept decreasing. At end-diastole, the aortic root had a truncated cone shape (base area > commissures area by 51.6 ± 2.0%). During systole, the root became more cylindrical (base area > commissures area by 39.2 ± 2.5%) because most of the significant changes occurred at commissural level (63.7 ± 3.6%). **Conclusion**: Aortic root expansion follows a precise chronology during systole and becomes more cylindrical – probably to maximize ejection. These findings might stimulate a more physiologic approach to aortic valve and aortic root surgical procedures.

Keywords: Aortic valve; Aortic root expansion; Dynamic anatomy

1. Introduction

Because valve replacement with prosthesis has been the standard treatment for aortic valve disease, detailed knowledge of the aortic valve and aortic root was not required. Recently, the increased use of pulmonary autografts, aortic homografts, stentless porcine valves, aortic valve repair or reconstruction, and valve-sparing procedures demands a better understanding of the functional anatomy of the aortic valve complex [1–8]. Although the importance of the sinuses of Valsalva (SoV) as part of the aortic valve was already intuitively shown by Leonardo da Vinci [9], aortic valve dynamics as part of the root have not been studied until recently. Aortic root expansion at the commissural level was originally described by Brewer et al. [10] in 1976, as an essential part of the aortic valve opening mechanism to reduce shear stress on the leaflets. Thubrikar et al. [11,12] described that this expansion was initiated prior to ejection. Further information on deformational dynamics and torsion of the aortic root has been recently described by Dagum et al. [13]; however, all studies have been limited by their data sampling rate (60 Hz), resulting in controversial conclusions. The purpose of this study was to clarify ambiguity from previous studies. Simultaneous recording of three-dimensional (3-D) sonomicrometry (200 Hz = 200 data points/s) and left ventricular (LV) and ascending aorta pressures allowed a continuous correlation between aortic root expansion at each phase of the cardiac cycle [14–16].

2. Materials and methods

Eight adult sheep (43 ± 2 kg) (mean ± SEM) underwent implantation of 15 ultrasonic crystals in the aortic root using cardiopulmonary bypass (pump time, 158 ± 8 min; cross clamping time, 75 ± 3 min).

* Corresponding author. Tel.: +1-406-329-5668; fax: +1-406-329-5880.
E-mail address: duran@saintpatrick.org (C.M.G. Duran).

1010-7940/02/$ - see front matter
PII: S1010-7940(02)00405-0

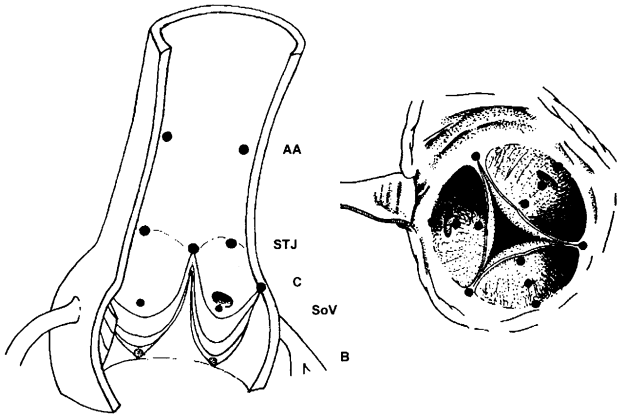

Fig. 1. Location of the sonomicrometry crystals in the aortic root. B, base; SoV, sinus of Valsalva; C, commissures; STJ, sinotubular junction; AA, ascending aorta.

2.1. Surgical protocol

Anesthesia was induced with i.v. ketamine 1.0 mg/kg and propofol 4.0 mg/kg body weight and was maintained with endotracheal isoflurane 1.5–2.5%. The EKG was monitored continuously. Artificial ventilation was achieved with a volume-regulated respirator (North American Drager, Telford, PA, USA) supplemented with oxygen at 2 l/min.

The heart was exposed with a standard left thoracotomy through the fourth intercostal space. The left femoral (16 Fr) and left internal thoracic (10 Fr) arteries were cannulated. A venous cannula was inserted into the right atrium (32 Fr). The aorta and a single arch vessel were cross-clamped, and cold crystalloid cardioplegia was infused into the root. To study the aortic valve complex, 15 ultrasonic crystals (Sonometrics Corp., London, Ontario, Canada) were implanted through a transverse aortotomy approximately 1 cm distal to the sinotubular junction. To avoid interoperator variability, the same surgeon placed all crystals. One millimeter ultrasonic crystals were placed and secured with 5/0 polypropylene sutures at: the lowest point of each sinus of Valsalva, corresponding to the so-called aortic base (B); the aortic commissures (C); the highest point of each supra-aortic crest or sinotubular junction (STJ), and at the wall of the ascending aorta (AA) (Fig. 1). On the ascending aorta, a left, right, and non-coronary (NC) crystal were lined up with the crystals placed at the left, right, and NC of the base and at the sinotubular junction. In four sheep, three crystals were placed on the concavity (deepest point) of the three SoV, and lined up between the crystals at the base and sinotubular junction. The crystals were oriented so that they all pointed toward the lumen. The crystal's electrodes were exteriorized through the aortic wall at each point of insertion to reduce their possible interference with the aortic valve movements. A needle with a slightly smaller diameter than the wire of the crystals was used to reduce the risk of a tear in the aortic wall. In case of bleeding, hemostasis was achieved with a 6/0 prolene suture. No deterioration of the signal transmission was noted. High-fidelity, catheter-tipped pressure transducers (model 510, Millar Instruments, Houston, TX, USA) were placed in the proximal ascending aorta and in the left ventricle through its apex.

2.2. Experimental design

After discontinuing cardiopulmonary bypass, and once the animal was hemodynamically stable (at least 15 min), recordings were taken at 200 Hz. Epicardial echocardiography with color Doppler was used to assess the competence of the aortic valve. At the end of the experiment, the heart was arrested by lethal injection of potassium chloride, explanted, and the correct position of the crystals was checked. All animals received humane care in compliance with the principles of the Animal Welfare Act, the *Guide for Care and Use of Laboratory Animals* from the US Department of Agriculture, and the Institutional Animal Care and Use Committee of the University of Montana.

2.3. Definition of the different phases of the cardiac cycle

The aortic root geometric changes were time related to each phase of the cardiac cycle, which was defined from the aortic and LV pressure tracings (Fig. 2) [17,18]. End-diastole or beginning of systole (beginning of isovolumic contraction) was defined as the beginning of LV pressure increase ($dP/dt > 0$). The end of isovolumic contraction was defined as the beginning of ejection at the crossing point of the LV and aortic pressure tracings (gradient aortic/LV pressure = 0). The dicrotic notch in the aortic pressure curve defined end-ejection. End of isovolumic relaxation was defined as the lowest point of LV pressures after ejection ($dP/dt = 0$) [13].

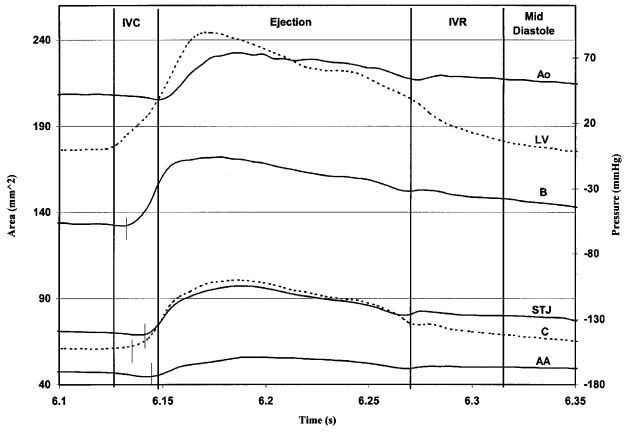

Fig. 2. Dynamic changes at the different levels of the aortic root time related to left ventricular and ascending aorta pressures. B, base; C, commissures; STJ, sinotubular junction; AA, ascending aorta; Ao, aortic pressure; LV, left ventricular pressure. Note the uniform cyclic deformation of the aortic root at each level during ejection and the precise order of expansion of the aortic root during isovolumic contraction (Sheep 7).

2.4. Definition of anatomic aortic root regions

The aortic root and the ascending aorta were divided into five cross-sectional areas defined by three crystals each: basal, commissural, sinotubular junction, sinus of Valsalva, and ascending aorta area (Fig. 1). The NC-right, right-left, and left-NC basal lengths were defined as the distances between each pair of basal crystals.

2.5. Data acquisition and calculation of aortic root deformation

Sonometrics Digital Ultrasonic Measurement System TRX Series 1 mm transmitter/receiver crystals were used to measure displacements. A post-processing program (Sonometrics Corp., London, Ontario, Canada) was used to examine each individual length tracing between crystals and for 3-D reconstruction of the crystal coordinates. All distances and pressures were synchronized with the EKG and recorded at the same time line on the same screen by the Sonometrics system.

Length data were obtained directly from the measured distances between a pair of crystals, and Lagrangian strain was used to define the deformation from the original length at end-diastole [19]. Each level of the aortic root was represented by a triangular area defined from the three corresponding crystals and calculated using Heron's formula [20]. A post-processing program, Sonovol (Sonometrics Corp., London, Ontario, Canada), was used to calculate aortic root volumes using the convex hull approach. The crystals at the base, sinotubular junction, and commissures were used for these calculations.

Changes in length, area, and volume were defined by: (1) total percentage change with reference to the original value at end-diastole; and (2) proportional percentage changes during each phase of the cardiac cycle relative to the total changes over the entire cycle.

2.6. Measurement and statistical analysis methods

After close examination of the data, three consecutive heartbeats that contained the least amount of noise were chosen for analysis. The summary statistics are reported as mean ± 1 standard error of the mean (SEM). Area changes at the different levels of the aortic root were tested for significance using Student's *t*-test for paired observation (significance level $P < 0.05$). Univariate generalized linear model (GLM) statistical methods were used to test for significant differences. The significance level used was 0.001. The expansion of the base, commissures, sinotubular junction, and ascending aorta were examined in an attempt to find a consistent expansion order. These results were displayed in a side-by-side boxplot. All statistical analyses were done using the SPSS 0.9 program (SPSS, Inc., Chicago, IL, USA).

3. Results

3.1. Model characteristics

At the time of recording, hemodynamic conditions were: heart rate (mean ± 1 SEM) 145 ± 8 min^{-1}, aortic pressure 70/45 ± 5/4 mmHg, stroke volume 20 ± 2 ml, and cardiac output 2.8 ± 0.3 l/min. Seven sheep had no regurgitation, and one had trivial regurgitation on epicardial echocardiographic control. In all necropsy checks, all crystals were in the correct position except for the deepest point of the sinus of Valsalva, where the crystals were often closer to the base than the sinotubular junction.

3.2. Baseline anatomy at end-diastole

At end-diastole, the aortic root was cone-shaped: the area of the base was larger than that of the commissures and sinotubular junction area by 51.6 ± 2.0 and 48.8 ± 3.9%, respectively. The disproportion between each level had a tendency to decrease during ejection so that the shape of the aortic root became more cylindrical (Fig. 3; Tables 1 and 2).

3.3. Aortic root dynamics during the cardiac cycle

During the cardiac cycle, the aortic root volume increased

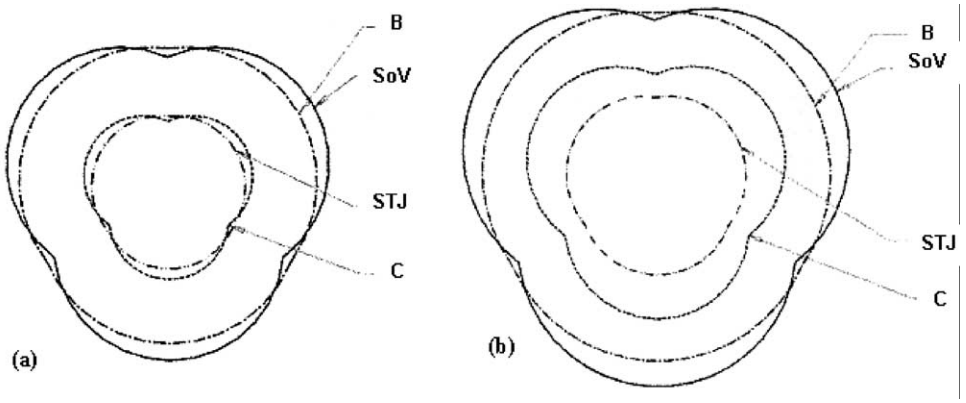

Fig. 3. Relative cross-sectional area diagram of the aortic root at end-diastole (a) and at maximum expansion (b) during ejection. B, base; SoV, sinus of Valsalva; STJ, sinotubular junction; C, commissures.

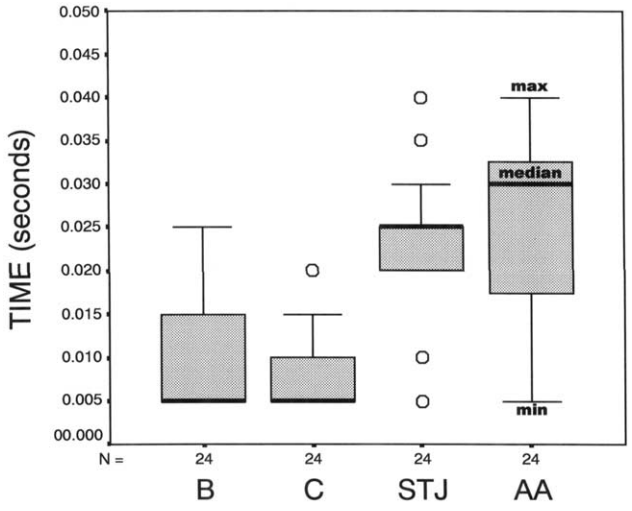

Fig. 4. Order of expansion at each level of the aortic root during isovolumic contraction. The results are displayed in a side-by-side box plot corresponding to three cardiac cycles for each of the eight sheep ($n = 24$). The thick, horizontal tracing in each box corresponds to the median value; the open circles correspond to five outlier measurements. Note that: (1) the median of the beginning of expansion of the base (B) and commissures (C) were similar; (2) the median of expansion of the sinotubular junction (STJ) and the ascending aorta (AA) were delayed toward the end of isovolumic contraction; and (3) the outliers correspond to the transition area of the STJ.

by a total of 33.7 ± 2.7%. Aortic root expansion started during isovolumic contraction, first at the base and commissures, followed by the sinotubular junction, and then the ascending aorta (Figs. 2 and 4). The aortic root reached maximal expansion during the first third of ejection, followed by a slow, then a late, rapid decrease in volume until mid-diastole. The maximum area changes occurred at commissural level (63.7 ± 3.6%) compared with the base (29.8 ± 3.3%) and the sinotubular junction (37.1 ± 2.1%). During end-diastole, aortic root volume re-expanded, but with different dynamics at each level: the basal and commissural areas re-expanded, whereas the sinotubular junction and ascending aorta areas kept decreasing (Table 2).

3.4. Aortic root anatomy during isovolumic contraction

Aortic root expansion started prior to ejection. Of the total aortic root volume increase, 36.7 ± 3.3% occurred during isovolumic contraction. During this phase, the aortic root started to expand at the base and the commissures, followed by the sinotubular junction and then the ascending aorta. It must be noted that the median of the beginning of expansion at the base and the commissures was similar; whereas the beginning of expansion of the sinotubular junction and ascending aorta was delayed to the second-half of isovolumic contraction (Fig. 4). In proportion, the expansion was larger at basal level (50.7 ± 4.5%) than at the commissures (32.8 ± 3.2%) (Table 2). Before the ascending aorta area started to increase (6.6 ± 1.0%) at the end of isovolumic contraction, it decreased by −2.6 ± 0.4%. SoV data were only available for four sheep and were recorded separately from the other crystals. Therefore, it was not possible to time relate SoV data with the other levels of the aortic root.

3.5. Aortic root anatomy during ejection

Ejection was divided into two phases: (1) a first third of ejection, where maximal aortic root expansion occurred; and (2) the last two-thirds of ejection, when the aortic root volume decreased (Fig. 2, Table 2).

During the first third of ejection, the aortic root reached maximal area expansion at each root level. The diameter ratio (Table 1) and area between the commissures and the sinotubular junction changed during ejection. At end-diastole, the commissural area was smaller (−3.4 ± 4.5%) than the sinotubular junction area; although during ejection, the commissural area became larger (15.1 ± 3.3%) than sinotubular junction area. Thus, during ejection, the aortic root had a tendency to change from a clover-shaped cone to a more cylindrical shape (Fig. 3). The diameter ratio (Table 1) and the area between the basal and the commissural level were also reduced during ejection. At end-diastole, the basal area was larger (51.6 ± 2.0%) than the commissural area; although during ejection, it was only larger by 39.2 ± 2.5%. Thus, during ejection, the aortic root had a tendency to become less cone-shaped and more cylindrical (Fig. 3).

Although the three lengths between each pair of basal crystals expanded during ejection, their capacity of expansion was significantly different ($P < 0.001$). The distance between the right and left basal crystals expanded by 19.2 ± 2.0%, the left-NC expanded by 12.9 ± 2.0%, and the NC-right by 8.4 ± 0.8%. In other words, the septal portion of the aortic root base (NC-right) expanded the

Table 1
Relative estimated diameter and ratio (related to basal diameter) at each level of the aortic root at end-diastole and at maximal expansion during the first third of ejection

	End-diastole		Ejection	
	Diameter (mm)	Ratio	Diameter (mm)	Ratio
Ascending aorta	13.7 ± 0.5	0.66	15.2 ± 0.5	0.66
Sinotubular junction	14.4 ± 0.4	0.69	16.7 ± 0.4	0.73
Commissures	14.1 ± 0.2	0.68	17.7 ± 0.2	0.77
Sinus of valsalva ($n = 4$)	20.4 ± 0.1	0.98	23.7 ± 0.3	1.03
Base	20.7 ± 0.4	1	22.9 ± 0.3	1

Table 2
Phase-related changes at each level of the aortic root for each phase of the cardiac cycle[a]

	IVC	Ejection (first third)	Ejection (last two-thirds)	IVR	Mid-diastole	End-diastole	Total expansion
Base (%)	50.7 ± 4.5*	49.2 ± 4.5*	−54.4 ± 2.0*	−44.1 ± 3.8*	−18.9 ± 1.5*	17.5 ± 3.0*	29.8 ± 3.3*
Area (cm^2)	1.45 ± 0.12	1.63 ± 0.09	1.45 ± 0.11	1.30 ± 0.12	1.24 ± 0.12	1.29 ± 0.12	1.63–1.29
Sinus of valsalva (%)	35.8 ± 4.8*	64.2 ± 4.8*	−74.9 ± 3.8*	−31.0 ± 2.2*	−6.3 ± 1.5*	12.2 ± 2.4*	38.4 ± 1.1*
Area (cm^2)	1.44 ± 0.08	1.76 ± 0.07	1.40 ± 0.08	1.24 ± 0.07	1.21 ± 0.06	1.27 ± 0.04	1.76–1.27
Commissures (%)	32.8 ± 3.2*	67.1 ± 3.2*	−66.6 ± 1.4*	−29.4 ± 1.2*	−8.6 ± 1.1*	4.7 ± 0.9*	63.7 ± 3.6*
Area (cm^2)	0.72 ± 0.05	0.98 ± 0.05	0.73 ± 0.04	0.62 ± 0.04	0.59 ± 0.04	0.60 ± 0.03	0.98–0.60
Sino-tubular junction (%)	13.8 ± 1.9*	86 ± 1.9*	−68 ± 2.6*	−14.2 ± 2.3*	−17.5 ± 2.7*	−0.2 ± 0.6*	37.1 ± 2.1*
Area (cm^2)	0.65 ± 0.07	0.85 ± 0.09	0.70 ± 0.08	0.67 ± 0.08	0.62 ± 0.07	0.62 ± 0.07	0.85–0.62
Ascending aorta (%)	6.6 ± 1.0*	93.3 ± 1.0*	−64.3 ± 3.0*	−10.9 ± 3.2*	−18.2 ± 3.6*	−6.4 ± 2.4*	26.3 ± 0.9*
Area (cm^2)	0.60 ± 0.09	0.74 ± 0.10	0.64 ± 0.09	0.63 ± 0.09	0.60 ± 0.09	0.59 ± 0.09	0.74–0.59
Aortic root volume (%)	36.7 + 3.3*	63.3 ± 3.3*	−53.1 ± 1.3*	−39.1 ± 3.6*	−19.0 ± 2.4*	11.3 ± 2.4*	33.7 ± 2.7*

[a] Data are displayed as: (1) percentage of area changes for each phase of the cardiac cycle relative to the total changes over the entire cycle; (2) raw area value measured at the end of each phase of the cardiac cycle. Results are expressed as mean ± 1 SEM (*$P < 0.05$).

least during systole, whereas the aortomitral junction or intertrigonal distance (corresponding to the left-NC basal length) underwent a larger expansion (12.9 ± 2.0%). During the last two-thirds of ejection, the aortic root volume decreased dramatically. The initial decrease was slow, followed by a rapid decrease at each area level (Table 2, Fig. 2).

3.6. Aortic root anatomy during diastole

A dicrotic notch was identified on each area curve at end-ejection. Diastole was divided into two phases: (1) a first-half until mid-diastole, when the aortic root decreased at all levels, and (2) an aortic root re-expansion during end-diastole (11.3 ± 2.4%). The dynamics of this re-expansion were different at each level. Although the basal (17.5 ± 3%) and commissural (4.7 ± 0.9%) areas re-expanded, the sino-tubular junction (−1.5 ± 0.6%) and ascending aorta (−6.4 ± 2.4%) areas kept decreasing (Table 2).

4. Discussion

Brewer et al. [10] pioneered the field of aortic root dynamic anatomy in 1976 by describing a 16% radial displacement of the commissures on an isolated aortic root model. Later, Thubrikar et al. [11,12], using three commissural radio-opaque markers in dogs, described aortic root expansion to be prior to ejection. Limited by their data-sampling rate of 60 images/s, their conclusions had to be based on abnormal cardiac cycles using the approximation that a non-ejecting extra systole was the equivalent to the isovolumic contraction phase. The advent of sonomicrometry, with a data acquisition rate of 200 Hz made our study of the actual aortic root volume changes during the normal cardiac cycle possible. The root increased its volume by 37.7 ± 2.7%, with 36.7 ± 3.3% of it occurring during the isovolumic contraction. Although the most significant changes occurred at the commissural level during systole, it was the base that, in proportion, expanded the most during the isovolumic contraction. These findings suggest that not only the commissural but also the basal expansion might initiate the opening of the aortic leaflets before ejection. Confirmation of this mechanism must await a parallel study that includes leaflet markers.

In 1988, Van Renterghem et al. [21] described basal strains in dogs using coils and a video-fluoroscopy recording system. They described that during ejection, the basal segments adjoining the myocardium (NC-right and right-left basal lengths) shortened, whereas the aortomitral junction (left-NC basal length) lengthened. Despite a high sampling rate of 150 Hz, incomplete recordings and very noisy signals reduced the number of valid data. In our study, continuous recording at 200 Hz showed an expansion of all three basal lengths, but in significantly different proportions. The segments of the aortic root base corresponding to the septum, i.e., the NC-right, expanded less

than the aortomitral junction or intertrigonal distance corresponding to the NC-left basal length. This surprising mobility of the aortomitral area during the cardiac cycle raises the question of the possible negative effects on the aortic mechanics when the mitral valve annulus is fixed by a rigid prosthesis.

Recently, Dagum et al. [13] described the time-related deformational dynamics of the aortic root during the cardiac cycle by using six video-fluoroscopic markers (three basal and three commissural) in an ovine model. This study assumed that the commissures and the crests of the sinotubular junction are in the same plane and, therefore, undergo the same deformation. Anatomically and histologically, the sinotubular junction is curvilinear, starting proximally at the commissures and curving upward along the supra-aortic crests [22,23]. In fact, the curved sinotubular junction is the distal limit of the SoV. In our study, the three crystals defining the plane of the sinotubular junction only correspond to highest point of the supra-aortic crests. According to our data, the dynamics of the commissures and sinotubular junction were different during isovolumic contraction and end-diastole. These findings suggest the presence of two different mechanisms in the expansion of the aortic root: a myocardial-related mechanism that includes the basal and commissural crystals, and an aortic-related mechanism that includes the sinotubular and aortic crystals. These findings corroborate the anatomic studies of Sutton et al. [22,23] that consider the aortic valve annulus as formed by the three interleaflet triangles rather than the scalloped line of attachment of the aortic leaflets. These interleaflet triangles, with apex in the commissures and sides corresponding to the line of leaflet attachment, seem to play a definite role in the mechanism of root expansion. Probably, the surgical concept of equating the aortic valve annulus as the scalloped line of insertion of the leaflets should be changed to the functional subaortic region proposed by Anderson's group [22,23].

We agree with Green et al. [24], who described a cylindrical dilatation of the aortic root (basal and commissural expansion) during isovolumic contraction – possibly to accommodate a greater pre-ejection LV volume to maximize ejection. This LV outflow tract volume redistribution remains speculative as a mechanism of root expansion; although a recent study of cardiac flow using magnetic resonance velocity mapping supports this continuous change within the LV [25]. A possible different mechanism for this systolic root expansion has been proposed by Vesley [26], who considers it a passive action when the pressure difference across the aortic valve is reduced. Dagum et al. [13] also described an annular (basal) contraction during ejection. Our data show that although the commissures expanded more than the base, the base area was still larger than the commissural area during the first third of ejection, where both reached maximal expansion. This cylindrical expansion became more obvious during ejection. The lower sampling rate (60 Hz) and lack of an aortic pressure that resulted in an imprecise definition of the beginning and end of ejection might explain the differences between our results and those of Dagum et al. The standard physiologic definition of the beginning ejection (end of isovolumic contraction) is when the aortic/LV pressure equalizes, and ejection ends at the dicrotic notch in the aortic pressure tracing [17,18]. Absence of aortic pressure data forced these authors to use imprecise, alternative methods to define ejection. At a low data-sampling rate of 0.0167 s (60 Hz), it is likely that the first third of ejection, where the base continued to expand, might have been integrated into the isovolumic contraction or not recorded. As a result, only the last two-thirds of ejection (when the base area decreased) were recorded (and therefore interpreted) as annular contraction during ejection.

The same problem might have occurred with the definition of the end of ejection, as they used the video-fluoroscopic frame preceding maximum negative dP/dt. At the beginning of our study, we used the same definition, but soon realized that maximum negative dP/dt did not correspond to end ejection; rather, it occurred in the last third of ejection, long before the dicrotic notch. Therefore, when Dagum et al. [13] described an early diastolic commissural re-expansion, it might have been the dicrotic notch that we observed in the area curves at each aortic root level.

In summary, aortic root expansion starts prior to ejection and follows a precise order. Each root level reached maximal expansion during the first third of ejection. Significant dynamic differences were detected between the basal and commissural levels and the sinotubular junction and ascending aorta levels. These different behaviors suggest different mechanisms of expansion. The differences in expansion at each level contribute to change the aortic root from a clover or conical shape during diastole to a more circular and cylindrical shape during systole. It can be speculated that these chronologic, geometric changes are the mechanism to maximize ejection. Better understanding of the aortic root dynamic anatomy should make us question and review our present surgical procedures on the aortic valve and aortic root. Prosthetic replacement of the aortic valve and aortic root with rigid structures completely destroys this delicate mechanism. The durability of the available stentless valves will also most likely be limited by their relative stiffness. Newer and more physiologic solutions are required.

4.1. Limitations of the study

The main limitation of this study is the invasive, acute, and open-chest nature of our model. Also, the deleterious effect of cardiopulmonary bypass and ischemia might have resulted in abnormal valve behavior. Furthermore, it can be argued that the high heart rate present at the time of data acquisition (probably due to catecholamine release) might alter aortic root motion recorded during the shorter cardiac cycles. No autonomic blockade was used to avoid LV function depression. The blood pressure at recording was lower

by 10–20 mmHg compared with pre-bypass measurements. Therefore, the expansion of the aortic root might have been underestimated compared with normal physiologic conditions. The constant patterns found in all animals and the fact that all geometric changes were related to the cardiac phases advocates for the validity of our findings. The possible source of error due to the presence of crystals and attached electrodes is inherent to all marker techniques. The aortic root electrodes were passed through the aortic wall at each location (outside the aortic lumen). Furthermore, variability in the precise location of the crystals must be considered. To help minimize this potential problem, all surgeries were performed by the same individual. Also, the calculated areas and volumes were based on only three crystals at each level of the root, which does not correspond to the more circular geometry of the natural root. This limitation would minimize the actual figures, but not the observed percent changes. Finally, findings in sheep are not necessarily applicable to the human. Anatomic differences due to bipedalism, such as the presence of the septal muscle shelf in sheep and species differences in sinus sizes and tissue compliance might influence the results.

Acknowledgements

We wish to thank Kathleen Billington and Leslie Trail for their effort and support that were essential to the completion of these experiments. We would also like to thank Reed Mandelko for providing illustrations for the paper and Jill Roberts for her editorial assistance.

References

[1] Ross DN. Replacement of the aortic and mitral valves with a pulmonary autograft. Lancet 1967;2:956–958.
[2] Duran CG, Gunning AJ. A method for placing a total homologous aortic valve in the subcoronary position. Lancet 1962;2:488–489.
[3] Angell WW, Pupello DF, Bessone LN, Hiro SP. Universal method for insertion of unstented aortic autografts, homografts and xenografts. J Thorac Cardiovasc Surg 1992;103:642–648.
[4] Duran C, Kumar N, Gometza B, Al Halees Z. Indications and limitations of aortic valve reconstruction. Ann Thorac Surg 1991;52:447–453.
[5] Duran CMG, Gometza B, Kumar N, Gallo R, Martin-Duran R. Aortic valve replacement with free hand autologous pericardium. J Thorac Cardiovasc Surg 1995;110:511–516.
[6] David TE. Aortic root aneurysms: remodeling or composite replacement? Ann Thorac Surg 1997;64:1564–1568.
[7] Yacoub MH, Gehle P, Chandrasekaran V, Birks EJ, Child A, Radley-Smith R. Late results of a valve sparing operation in patients with aneurysm of the ascending aorta and root. J Thorac Cardiovasc Surg 1998;115:1080–1090.
[8] Leyh RG, Schmidtke C, Sievers HH, Yacoub MH. Opening and closing characteristics of the aortic valve after different types of valve-preserving surgery. Circulation 1999;100:2153–2160.
[9] Robicksek F. Leonardo da Vinci and the sinuses of Valsalva. Ann Thorac Surg 1991;52:328–335.
[10] Brewer RJ, Deck JD, Capati B, Nolan SP. The dynamic aortic root: its role in aortic valve function. J Thorac Cardiovasc Surg 1976;72:413–417.
[11] Thubrikar M, Harry L, Nolan SP. Normal aortic valve function in dogs. Am J Cardiol 1977;40:563–568.
[12] Thubrikar M, Bosher LP, Nolan SP. The mechanism of opening of the aortic valve. J Thorac Cardiovasc Surg 1979;77:863–870.
[13] Dagum P, Green P, Nistal FJ, Daughters GT, Timek TA, Foppiano LE, Bolger AF, Ingels Jr NB, Miller DC. Deformational dynamics of the aortic root: modes and physiologic determinants. Circulation 1999;100(Suppl II):II54–II62.
[14] Gorman III JH, Gupta KB, Streicher JT, Gorman RC, Jackson BM, Ratcliffe MB, Bogen DK, Edmunds Jr LH. Dynamic three-dimensional imaging of the mitral valve and the left ventricle by rapid sonomicrometry array localization. J Thorac Cardiovasc Surg 1996;112:712–726.
[15] Hansen B, Menkis AH, Vesely I. Longitudinal and radial distensibility of the porcine aortic root. Ann Thorac Surg 1995;60:S384–S390.
[16] Pang DC, Choo SJ, Luo HH, Shomura Y, Daniel S, Nikolic SJ, Cheung DT, Oury JH, Duran CMG. Significant increase of aortic root volume and commissural area occurs prior to aortic valve opening. J Heart Valve Dis 2000;9:9–15.
[17] Guyton AC, Hall JE. Textbook of medical physiology. 9th ed. Philadelphia: Saunders, 1996 p. 110–5.
[18] Mountcastle VB. Medical physiology. 13th ed., Saint Louis: Mosby, 1974 p. 892–3.
[19] Fung YC. Biomechanics: motion, flow, stress, and growth. New York: Springer, 1990 p. 358.
[20] Pappas T. Heron's Theorem. The joy of mathematics. San Carlos, CA: Wide World Publishing/Tetra, 1989 p. 62.
[21] Van Renterghem RJ, Van Steenhoven AA, Arts T. Deformation of the dog aortic valve ring during the cardiac cycle. Pflugers Arch 1988;412:647–653.
[22] Sutton JP, Ho SY, Anderson RH. The forgotten interleaflet triangles: a review of the surgical anatomy of the aortic valve. Ann Thorac Surg 1995;59:419–427.
[23] Anderson RH, Devine WA, Ho SY, Smith A, McKay R. The myth of the aortic annulus: the anatomy of the subaortic outflow tract. Ann Thorac Surg 1991;52:640–646.
[24] Green GR, Dagum P, Timek TA, Nistal F, Bolger AF, Daughters Jr GT, Ingels Jr NB, Miller DC. The mechanics of aortic valve opening in an ovine model. Circulation 1999;100:363 (abstract).
[25] Kilner PJ, Yang YZ, Wilkes AJ, Mohiaddin RH, Firmin DN, Yacoub MH. Asymmetric redirection of flow through the heart. Nature 2000;404:759–761.
[26] Vesely I. Aortic root dilatation prior to valve opening explained by passive hemodynamics. J Heart Valve Dis 2000;9:16–20.